

Investigating magnetic proximity effects in NiO/Pd with polarized neutron reflectometry

A. Hoffmann* and M. R. Fitzsimmons

Los Alamos National Laboratory, Los Alamos, New Mexico 87545

J. A. Dura and C. F. Majkrzak

National Institute of Standards and Technology, Gaithersburg, Maryland 20899

(Received 3 April 2001; published 19 December 2001)

With polarized neutron reflectometry we investigated NiO/Pd heterostructures for the presence of a magnetic proximity effect, which is expected to produce an induced ferromagnetic moment in Pd. Using a specific isotope mixture of Ni in the preparation of NiO, the chemical contrast across the Pd/NiO interface was greatly suppressed, thus enhancing sensitivity to magnetic contrast at the reflecting interface. Despite enhanced sensitivity, no evidence for a proximity effect was observed. If present, the magnetic moment per Pd atom could not be more than $0.01\mu_B$, regardless of Pd layer thickness, crystalline interface orientation, and number of NiO/Pd bilayers.

DOI: 10.1103/PhysRevB.65.024428

PACS number(s): 75.70.Cn

I. INTRODUCTION

The discovery of giant magnetoresistance¹ and its subsequent use in magnetic recording technology have renewed interest in magnetic heterostructures and the magnetic properties across interfaces of magnetically dissimilar materials.^{2,3} One question germane to studies of magnetic heterostructures is whether magnetic order in one material induces magnetic order in a nominally nonmagnetic material, giving rise to a so-called magnetic proximity effect. For example, easily polarizable materials, such as Pd and V (i.e., materials that are almost ferromagnetic), can acquire a sizable magnetic moment if they are in contact with a ferromagnetic material.⁴⁻⁹ Theoretical calculations suggest that the first layer of Pd in contact with a ferromagnetic material acquires a magnetic moment of about $0.3\mu_B$ /Pd atom, which then decays rapidly away from the interface.¹⁰

Recently Manago *et al.*¹¹⁻¹³ suggested that NiO/Pd superlattices can acquire a ferromagnetic moment. Since NiO is an antiferromagnet, and thus has no net magnetization, Manago *et al.* concluded the observed magnetization came from a ferromagnetic moment induced in Pd. By measuring a systematic variation of the observed magnetization with Pd layer thickness Manago *et al.* inferred a magnetic moment of $0.59\mu_B$ /Pd atom, which decayed away from the Pd/NiO interface to zero within 35 \AA .¹² However, neither the Pd magnetic moment nor the spatial dependence was observed directly in these experiments. The goal of this study was to directly observe the induced Pd moment and characterize its spatial dependence in NiO/Pd heterostructures by polarized neutron reflectometry—a technique tailor-made to accurately determine the depth dependence of the magnetization profile in a magnetic heterostructure.¹⁴ There are other methods such as magnetic dichroism which also have the necessary sensitivity and chemical specificity, but any spatial dependence is normally inferred indirectly, e.g., by varying layer thicknesses.⁸

II. ENHANCEMENT OF MAGNETIC CONTRAST

Within the optical formalism of Parratt,¹⁵ the reflectivity of a sample measured with polarized neutrons is related to

the variation of the index of refraction n for the sample averaged over its lateral dimensions. The index of refraction, n , is given by¹⁶

$$n^{\pm} = n_N \pm n_M = 1 - \frac{\lambda^2}{2\pi} [b(z)N(z) \pm 4\pi cM(z)], \quad (1)$$

where n_N and n_M are the nuclear and magnetic contributions, respectively, to the index of refraction, λ is the neutron wavelength [\AA], $b(z)$ is the averaged nuclear scattering amplitude [\AA] as a function of distance z from the surface, $N(z)$ is the atomic density [\AA^{-3}], $c = 2.645 \times 10^{-5} \text{ \AA} / \mu_B$ is a constant, and $M(z)$ is the magnetization density [$\mu_B \text{\AA}^{-3}$]. The \pm signs refer to the orientation of the neutron beam polarization relative to the applied magnetic field, either parallel (+ or up) or antiparallel (− or down).¹⁷ Using an iterative process¹⁵ and Eq. (1), the specular polarized neutron reflectivity R^{\pm} is calculated as a function of momentum transfer, $q = 4\pi \sin \theta / \lambda$, with θ being the angle between the incoming neutron beam and its projection on the sample surface.¹⁴ The reflectivity profiles $R^{\pm}(q)$ contain both information about the chemical profile [through the nuclear scattering length density $\beta(z) = b(z)N(z)$] and the magnetic profile [through the magnetic scattering length density $4\pi cM(z)$]. A net magnetic moment in the sample manifests itself by a splitting between the two reflectivity profiles, such that $R^+ \neq R^-$ if $M(z) \neq 0$.

Previously, polarized neutron reflectometry has been used to determine with 10% precision the net magnetic moment from ferromagnetic layers a few monolayers thick.^{18,19} This high sensitivity to a small magnetization volume was obtained by a judicious choice of an overlayer of similar nuclear scattering length as the substrate, so as to create a resonance (anti-resonance) for up (down) polarized neutrons, which then in turn gives rise to enhanced magnetic contrast.

The goal of the present experiment is to detect a magnetic moment of up to $0.6\mu_B$ /Pd atom, which could possibly extend from the Pd/NiO interface only 10–40 \AA into the Pd. This is preferably investigated in simple bilayer samples (with only one Pd/NiO interface), since it avoids problems

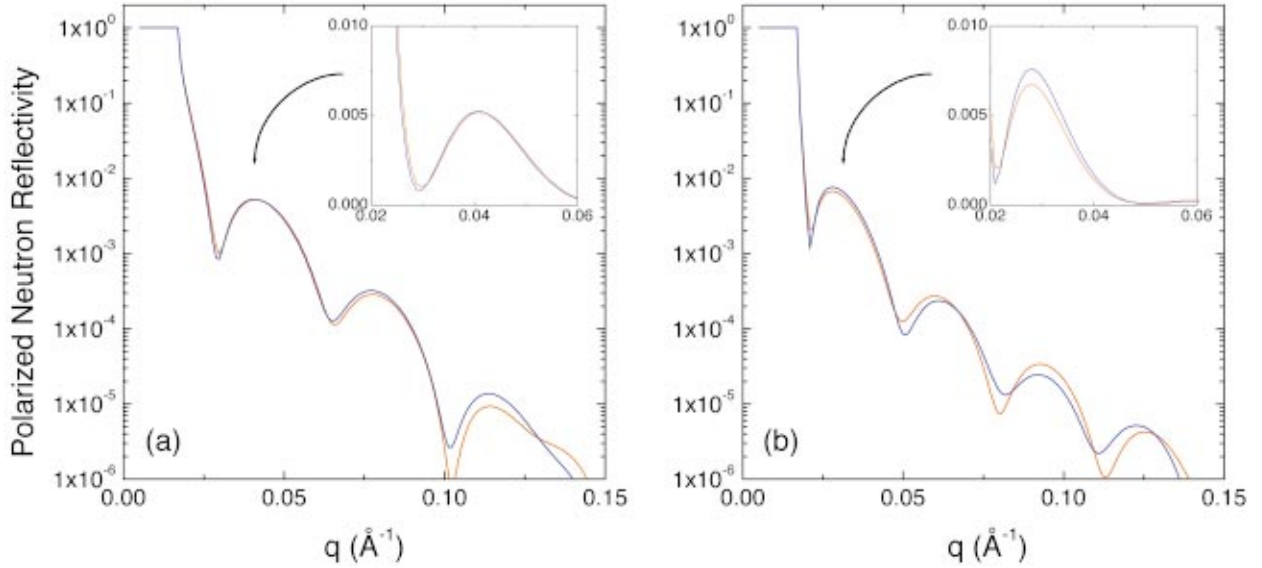


FIG. 1. (Color) Simulations of polarized neutron reflectivities for a bilayer of 50 Å NiO/150 Å Pd on a Al_2O_3 substrate; R^+ is red, R^- is blue. The simulation is shown for (a) NiO with natural abundance of Ni isotopes and (b) for NiO with a specific mixture of Ni isotopes as described in the paper. The insets show the first fringe maximum on a linear scale.

with inequivalent interfaces and simplifies the data analysis. Clearly, detection of such a small moment is a challenging problem and therefore we extended the idea of contrast matching from Ref. 18 to the present problem. Using specific isotopes of Ni, we can match the nuclear contrast throughout the heterostructure such that the nuclear scattering length density β is constant throughout our Pd/NiO bilayer system, i.e., $\beta_{\text{NiO}} = \beta_{\text{Pd}}$. Thus, chemical contrast across the Pd/NiO is suppressed with a concomitant enhancement in (relative) magnetic contrast. Notice that $\beta_{\text{Pd}} = 4.013 \times 10^{-6} \text{ \AA}^{-2}$ for natural Pd is smaller than $\beta_{\text{NiO}} = 8.840 \times 10^{-6} \text{ \AA}^{-2}$ for natural NiO. Since the scattering length density is given by $\beta = \bar{b}N$, where \bar{b} is the nuclear scattering amplitude averaged over all different atoms and isotopes and N is the atomic density, it is thus possible to achieve contrast matching by using an appropriate amount of ^{62}Ni , which has a negative scattering length of $b = -8.7 \times 10^{-5} \text{ \AA}$, compared to $b = 10.3 \times 10^{-5} \text{ \AA}$ for natural Ni.^{20,21}

To demonstrate enhanced magnetic contrast, reflectivity profiles were calculated for a bilayer composed of 50-Å-thick NiO and 150-Å-thick Pd on a MgO substrate with a moment in the Pd layer of $0.32\mu_B/\text{atom}$ decaying exponentially²² away from the Pd/NiO interface within 10 Å. These simulations suggest that a measurable difference between R^+ and R^- can be achieved using a special isotopic mixture of Ni. It should be pointed out that the induced magnetic Pd moment and its spatial extent used in our simulations are similar to what has been suggested for Pd/Fe bilayers,¹⁰ but significantly smaller than the values inferred by Manago *et al.*¹² For larger magnetic moments or spatial extent, such as the ones suggested by Manago *et al.*, the magnetic contrast would be even larger. Reflectivity profiles for a Pd/NiO bilayer using the natural abundance of Ni isotopes [Fig. 1(a)] and a special ^{62}Ni -enriched mixture [Fig. 1(b)] were calculated. Comparing these profiles a larger

splitting between R^+ and R^- especially at high reflectivities is observed for the ^{62}Ni -enriched composition. Since $M(z)$ is related to this splitting, use of the special isotope mixture offers significant benefits. In Fig. 1(b) the mixture of ^{62}Ni and natural Ni is such that the nuclear scattering length density of NiO is the same as Pd. In order to show the matching for the scattering length densities β of NiO and Pd, β is plotted in Fig. 2 for neutron beam polarization up (blue) and down (red) for natural Ni isotope abundance (a) and for the ^{62}Ni /natural Ni mixture (b).

III. SAMPLE PREPARATION AND CHARACTERIZATION

Several epitaxial NiO/Pd bilayers and superlattices were grown on [001] Al_2O_3 and on [100], [110], and [111] MgO substrates. By choosing different substrates, bilayers could be grown with different crystalline orientations. Thus, the influence of the interfacial antiferromagnetic spin structure on the magnetic proximity effect can be investigated. Notice also that, since the antiferromagnetic structure of NiO has ferromagnetically aligned layers along the [111] planes, a proximity effect in NiO/Pd is expected to be most enhanced for [111]-oriented NiO films.

Before film deposition, the substrates were heated to 500 °C for 1 h. The NiO was deposited by electron beam evaporation from a Ni target with a 1.18:1 ratio of ^{62}Ni and natural Ni in an oxygen atmosphere of 4×10^{-4} Torr while the substrate temperature was maintained at 200 ± 2 °C. Subsequently, the substrates were cooled to room temperature, and the oxygen evacuated so that the base pressure before deposition of Pd from a 99.99% pure target was $< 10^{-7}$ Torr. The deposition rate of NiO and Pd was 0.6 Å/s. For the preparation of NiO/Pd superlattices the substrate temperature was maintained at 200 ± 2 °C throughout film growth. Prior

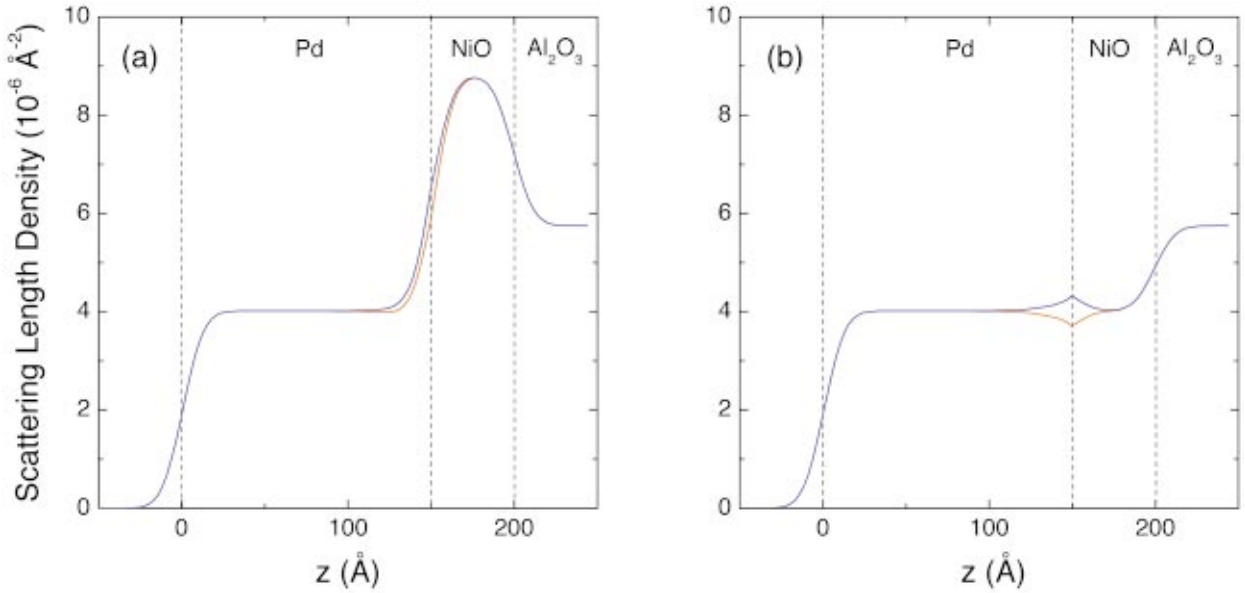


FIG. 2. (Color) Scattering length densities as a function of depth z into the film used for the simulations shown in Fig. 1 (red line for neutron beam polarization down, blue line for up): (a) with natural abundance of Ni isotopes and (b) with a specific isotope composition of Ni in order to adjust the nuclear scattering length in NiO to the one of Pd. The dashed lines indicate the positions of the various interfaces.

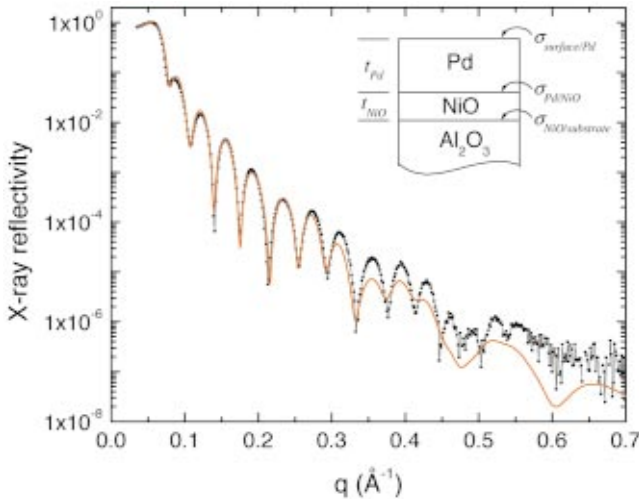


FIG. 3. (Color) X-ray reflectivity of 46.5 \AA NiO/ 154.3 \AA Pd on a $[001] \text{ Al}_2\text{O}_3$ substrate (black dots) and fit to the data (red solid line). The inset shows the fitting parameters, which are also listed in Table I.

to deposition of Pd, oxygen used to grow NiO layers was evacuated from the electron beam evaporator.

The crystal and chemical structure of the NiO/Pd samples was extensively characterized with x-ray diffraction and x-ray reflectometry. Figure 3 shows the x-ray reflectivity for a NiO/Pd bilayer grown on $[001] \text{ Al}_2\text{O}_3$, which is used to determine the chemical layer structure including interfacial roughness. This information will be used later as fixed parameters for the model used for fitting the neutron reflectivities. A fit of the data obtained using a model structure and an iterative algorithm¹⁵ is shown in Fig. 3 with a red solid line. The structural parameters for the NiO/Pd bilayer obtained from the fit to the x-ray reflectivity are shown in detail in Table I for one series of four samples (including the one whose data is shown in Fig. 3) deposited simultaneously on various substrates. Note all Pd/NiO interfaces are very sharp regardless of crystal orientation or substrate.

The high-angle x-ray diffraction pattern for the same NiO/Pd bilayer on $[001] \text{ Al}_2\text{O}_3$, whose low-angle profile was discussed previously, is shown in Fig. 4. From high-angle

TABLE I. Structural parameters obtained from fitting the x-ray reflectivities for NiO/Pd bilayers grown on $[001] \text{ Al}_2\text{O}_3$, $[100]$, $[110]$, and $[111] \text{ MgO}$. Listed are the NiO (t_{NiO}) and the Pd (t_{Pd}) layer thicknesses, as well as the roughnesses of each interface $\sigma_{\text{surface/Pd}}$, $\sigma_{\text{Pd/NiO}}$, and $\sigma_{\text{NiO/substrate}}$ (see also the inset in Fig. 3). Additionally the full width at half maximum $\Delta\theta$ for the high angle Pd peaks $[(111)$, (200) , (220) , and (111) , respectively] is shown.

Substrate	$[001] \text{ Al}_2\text{O}_3$	$[100] \text{ MgO}$	$[110] \text{ MgO}$	$[111] \text{ MgO}$
$t_{\text{Pd}} [\text{\AA}]$	154.3 ± 0.2	132.3 ± 0.1	139.9 ± 0.2	156.9 ± 0.3
$t_{\text{NiO}} [\text{\AA}]$	46.5 ± 0.3	41.6 ± 0.4	44.9 ± 0.2	44.21 ± 0.05
$\sigma_{\text{surface/Pd}} [\text{\AA}]$	6.4 ± 0.2	4.44 ± 0.07	7.07 ± 0.03	7.3 ± 0.2
$\sigma_{\text{Pd/NiO}} [\text{\AA}]$	3.73 ± 0.07	3.28 ± 0.04	6.1 ± 0.1	4.35 ± 0.06
$\sigma_{\text{NiO/substrate}} [\text{\AA}]$	1.9 ± 0.2	3.9 ± 0.1	6.01 ± 0.08	3.95 ± 0.08
$\Delta\theta_{\text{Pd}} [\text{deg}]$	0.030 ± 0.001	0.84 ± 0.08	1.38 ± 0.05	0.058 ± 0.005

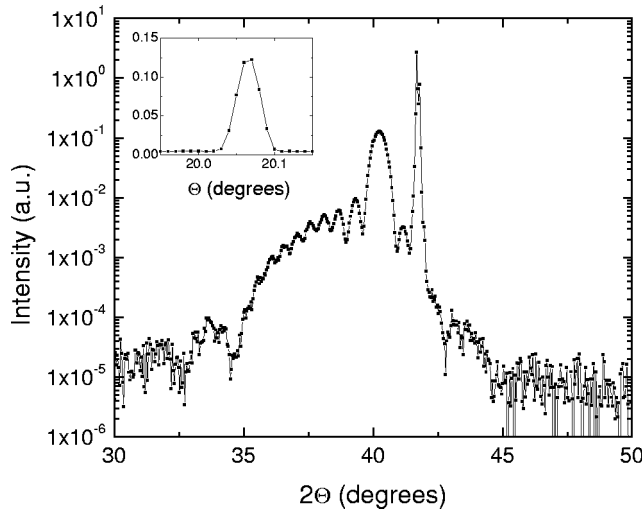


FIG. 4. High-angle x-ray diffraction of 46.5 Å NiO/154.3 Å Pd on [001] Al₂O₃. The inset shows the rocking curve of the Pd (111) peak.

x-ray diffraction data, the texture, mosaic spread, and phase purity of our samples were determined. Only the NiO (111) and Pd (111) Bragg peaks are observed, indicating the [111] texture of the bilayer. Furthermore, there are no peaks of any other phases besides Al₂O₃, NiO, and Pd. For both the (111) Pd and (111) NiO Bragg reflections there are distinct finite-size fringes, from which the thickness of each layer individually (157 ± 3 Å for Pd and 47 ± 10 Å for NiO) can be determined. These thicknesses agree very well with the thicknesses (see Fig. 3 and Table I) obtained from the x-ray reflectivity measurements. The inset of Fig. 4 shows the rocking curve of the (111) Pd Bragg peak, which indicates the low mosaic spread of the crystal planes perpendicular to the sample surfaces. Again, the high-angle data for the NiO/Pd bilayers grown on [100], [110], and [111] MgO are similar, showing [100], [110], and [111] texture, respectively, with no additional phases. However, the mosaic spread is somewhat larger as can be seen in Table I.

Grazing incidence in-plane x-ray diffraction was used to determine the in-plane crystal structural quality of the samples. A polar plot of the integrated in-plane (220) Pd reflection intensity as a function of azimuthal angle ω during rotation about the surface normal of the [111] oriented Pd film is shown in Fig. 5 for the NiO/Pd bilayer grown on [001] Al₂O₃. There is a clear sixfold symmetry, such that [220] Pd \parallel [300] Al₂O₃ (the Al₂O₃ diffraction peaks are not shown in Fig. 5 for the sake of clarity). The sixfold symmetry of the diffraction pattern indicates that both the Pd and the NiO layers grew epitaxially on [001] Al₂O₃.²³ All samples grown on the MgO substrates also showed equally good epitaxial quality.

To summarize the structural x-ray diffraction characterization, all samples were single-crystalline epitaxial NiO/Pd bilayers with minimal roughness and interdiffusion (below three monolayers). High quality samples were grown regardless of crystallographic orientation.

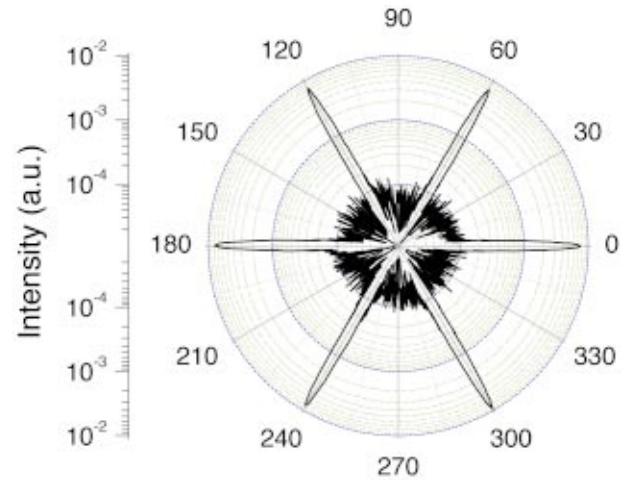


FIG. 5. (Color) Grazing-incidence x-ray diffraction of 46.5 Å NiO/154.3 Å Pd on [001] Al₂O₃. Shown is a polar plot of the in-plane (220) Pd Bragg intensity as a function of rotation about the film normal.

IV. POLARIZED NEUTRON REFLECTOMETRY

Polarized neutron reflectometry measurements were performed using the NG-1 reflectometer at the NIST Center for Neutron Research. Prior to measurement, each sample was cooled in a 2 kOe field from 300 K to 25 K. This cooling procedure was chosen since the earlier reports of Manago *et al.* suggested a T_c for the NiO/Pd system below 300 K.¹³ The neutron measurements were performed in an applied field ranging from 2 kOe to 7.5 kOe. The polarized neutron reflectivity measurements for the NiO/Pd bilayer on [001] Al₂O₃, whose x-ray data are shown in Figs. 3–5, is shown in Fig. 6(a). No obvious difference between the R^+ and R^- reflectivity profiles is observed, indicating that there is no significant net magnetic moment in the sample. Additional quantitative fitting [shown in Fig. 6(a) with the solid lines] further confirms that no net magnetic moment exists in this sample. The fits were obtained using an iterative algorithm¹⁵ and using the structural parameters obtained from the fits to the x-ray reflectivities (see Table I). The only fitted parameters were the nuclear scattering lengths for NiO and Pd and the net magnetic moment in the Pd layer, which was assumed to decay exponentially from the interface within 10 Å.²² With this assumption an induced magnetic Pd moment of $\mu_{Pd} = (0.003 \pm 0.008) \mu_B$ is obtained directly at the NiO/Pd interface. Thus an upper limit for an induced Pd moment is about $0.01 \mu_B/\text{atom}$. An even smaller moment would be required had the moment been distributed within a larger distance than 10 Å of the Pd/NiO interface. Results from samples prepared on MgO substrates were similar and also showed no evidence of any significant magnetic moment. Therefore, we conclude that there is no evidence for an induced moment in Pd regardless of the crystalline orientation of the NiO/Pd interface.

In addition to measuring the non-spin-flip reflectivities R^\pm we also measured the spin-flip reflectivities, which would indicate any magnetization component perpendicular to the applied magnetic field. It is possible that antiferromag-

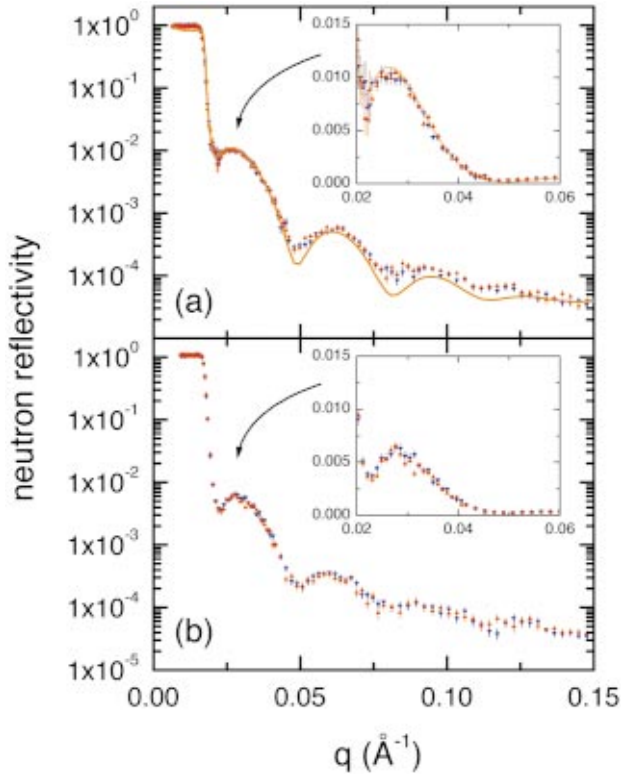


FIG. 6. (Color) Polarized neutron reflectometry for (a) 46.5 Å NiO/154.3 Å Pd and (b) 181 Å NiO/5.5 Å Pd on [001] Al₂O₃. Red data points are for R^+ , blue data points are for R^- . The statistical error bars are indicated by vertical lines. The orange and light blue solid lines in (a) are fits for R^{\pm} , respectively. The insets show the data at the first fringe maximum on a linear scale.

netic order in the antiferromagnetic layer gives rise to new anisotropies in an adjacent ferromagnetic layer.^{24,25} This could then give rise to a magnetization, which is not aligned with the applied field. However, we never observed any spin-flip scattering and thus did not observe any ferromagnetic moment in the spin-flip reflectivities either.

The fitted values for the nuclear scattering length densities of Pd and NiO were $\beta_{Pd} = (4.5 \pm 0.1) \times 10^{-6} \text{ \AA}^{-2}$ and $\beta_{NiO} = (4.1 \pm 0.2) \times 10^{-6} \text{ \AA}^{-2}$. The fitted values for β_{Pd} and β_{NiO} also correspond well to the published literature value²⁶ of the Pd nuclear scattering length density, $\beta'_{Pd} = 4.0 \times 10^{-6} \text{ \AA}^{-2}$. Thus, the nuclear scattering density of NiO was indeed well matched (to <10%) to the Pd nuclear scattering length density. Good matching is further demonstrated by the polarized neutron reflectometry measurements on a 181 Å NiO / 6 Å Pd bilayer on [001] Al₂O₃ [see Fig. 6(b)]. This sample has a similar overall thickness as the sample (154 Å NiO/47 Å Pd) previously discussed, but different Pd and NiO layer thicknesses. Note the reflectivity profiles shown in Figs. 6(a) and 6(b) are nearly identical, indicating the lack of chemical contrast between the NiO and Pd layers. Again there is no significant splitting between the two spin cross sections in Fig. 6(b) and thus no significant magnetic moment in the Pd layer, regardless of the Pd layer thickness.

Another example of the successful suppression of chemical contrast across the Pd/NiO is presented in Fig. 7, where

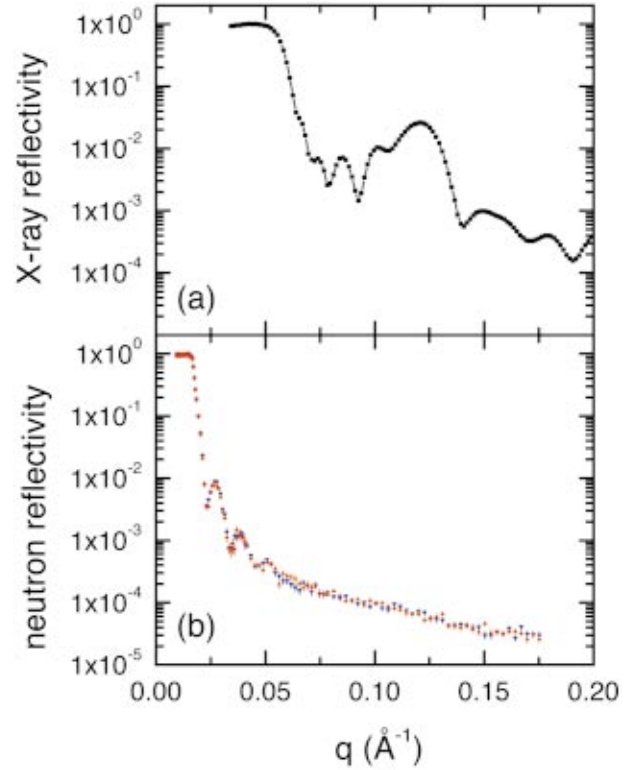


FIG. 7. (Color) (a) X-ray reflectivity for a (17 Å NiO/24 Å Pd)₁₀ superlattice on [001] Al₂O₃. (b) Polarized neutron reflectivity for a (17 Å NiO/24 Å Pd)₁₀ superlattice on [001] Al₂O₃. Red data points are for the R^+ , blue data points are for R^- . The statistical error bars are indicated by vertical lines.

x-ray (a) and polarized neutron (b) reflectivity profiles for a (17 Å NiO/24 Å Pd)₁₀ superlattice on [001] Al₂O₃ are shown. While the x-ray data show the first superlattice Bragg peak (at about 0.12 Å⁻¹), no such superlattice Bragg peak is observed in the neutron reflectivity data, indicating once again that the nuclear scattering length densities of NiO and Pd are well matched. Even though this superlattice sample has nominally the same structure (except for the number of bilayer repetitions) as the ones studied by Manago *et al.*,¹¹⁻¹³ no evidence for an induced magnetic moment was observed. The absence of any measurable magnetic moment for this superlattice was further confirmed by superconducting quantum interference device (SQUID) magnetometry measurements, which did not detect any significant magnetic moment.

Clearly, a discrepancy between our data and the earlier reported results by Manago *et al.*¹¹⁻¹³ exists. Specifically, the present results find no evidence for any significant ferromagnetic moment in samples of various crystalline orientations, thicknesses, and bilayer repetitions, even though the sensitivity of the neutron reflectometry is more than sufficient to detect a magnetic structure inferred by Manago *et al.* (see Sec. II). Therefore, we believe that the observations from Manago *et al.* are extrinsic in origin. One extrinsic origin could be a deviation of NiO from ideal stoichiometry, which can give rise to ferrimagnetic behavior.²⁷ Such a deviation

could also explain the unusual dependence of the measured magnetic moment on NiO layer thickness observed by Manago *et al.*¹¹ if, for example, ferromagnetic precipitates occur close to the NiO/Pd interface in the NiO layers. Recently Ohldag *et al.* have shown that under certain circumstances NiO can be reduced close to interfaces in magnetic heterostructures to form pure Ni.²⁸

Furthermore, it is interesting to note that Manago *et al.* observed the biggest ferromagnetic moments in samples with polycrystalline NiO. At the same time it is very well known that small particles and polycrystalline thin films of transition metal antiferromagnets can show a net magnetization due to uncompensated moments.^{29,30} This might also explain the absence of any observed magnetic moment in the epitaxially grown samples presented in this study.

One further difference between our samples and the ones studied by Manago *et al.* is the growth temperature, in particular for the Pd layer. The higher growth temperatures used by Manago *et al.* could give rise to increased interdiffusion, which could then give rise to a magnetic moment within the Pd layer.

There could be several reasons for the absence of any magnetic proximity effect for Pd grown on NiO. NiO develops antiferromagnetic domains even in single-crystal samples.³¹ These domains could induce moments in the Pd layer in various directions such that no long-range order can be established. The same effect could also occur due to structural defects, such as steps, which could give rise to an effective frustration of any proximity effect. Of course the absence of any proximity effect could also be more intrinsic—for example, due to the insulating nature of NiO. Since the electrons are localized in NiO, it could be that their influence on the Pd band structure is simply negligible.

V. CONCLUSION

We have shown that by matching the nuclear scattering length densities in magnetic heterostructures one can suppress chemical contrast across a reflecting interface, which can lead to enhanced sensitivity to magnetic contrast using polarized neutron reflectometry measurements. This technique is particularly beneficial in studies of very small magnetic moments confined to a few atomic layers. Suppression of chemical contrast was achieved for bilayers and superlattices of Pd and NiO prepared with a specific mixture of natural Ni and ⁶²Ni. Samples with different Pd and NiO thicknesses as well as several crystallographic orientations were examined. Despite excellent crystalline quality and successful efforts to suppress chemical contrast, no evidence for any induced moment in Pd was observed. In fact, by fitting the data an upper limit on any induced moment in Pd to $0.01\mu_B/\text{atom}$ was determined. We conclude that the Pd/NiO system does not show an intrinsic proximity effect and that previously observed ferromagnetic moments are probably extrinsic in nature.

ACKNOWLEDGMENTS

The neutron scattering facility of the National Institute of Standards and Technology is greatly appreciated. We would like to acknowledge D. Lederman, C. Leighton, and Ivan K. Schuller for many stimulating discussions. Furthermore, we would like to thank J. Thompson for assistance with magnetometry measurements. This work was supported by the U.S. Department of Energy, BES-DMS, under Contract No. W-7405-Eng-36. One of us (A.H.) thanks the Los Alamos National Laboratory for its support.

*Present address: Argonne National Laboratory, Materials Science Division, 9700 S. Cass Avenue, Argonne, IL 60439.

¹M. N. Baibich, J. M. Broto, A. Fert, F. Nguyen Van Dau, F. Petroff, P. Etienne, G. Creuzet, A. Friedrich, and J. Chazelas, *Phys. Rev. Lett.* **61**, 2472 (1988).

²For an extensive review see L. M. Falicov, D. T. Pierce, S. D. Bader, R. Gromsky, K. B. Hathaway, H. J. Hopster, D. N. Lambeth, S. S. P. Parkin, G. Prinz, M. Salamon, I. K. Schuller, and R. H. Victoria, *J. Mater. Res.* **5**, 1299 (1990).

³For a short review see I. K. Schuller, S. Kim, and C. Leighton, *J. Magn. Magn. Mater.* **200**, 571 (1999).

⁴F. J. A. den Broeder, H. C. Donkersloot, H. J. G. Draaisma, and W. J. M. de Jonge, *J. Appl. Phys.* **61**, 4317 (1987).

⁵Z. Celinski, B. Heinrich, J. F. Cochran, W. B. Muir, A. S. Arrott, and J. Kirschner, *Phys. Rev. Lett.* **65**, 1156 (1990).

⁶O. Rader, E. Vescovo, J. Redinger, S. Blügel, C. Carbone, W. Eberhardt, and W. Gudat, *Phys. Rev. Lett.* **72**, 2247 (1994).

⁷E. E. Fullerton, D. Stoeffler, K. Ounadjela, B. Heinrich, Z. Celinski, and J. A. C. Bland, *Phys. Rev. B* **51**, 6364 (1995).

⁸J. Vogel, A. Fontaine, V. Cros, F. Petroff, J.-P. Kappler, G. Krill, A. Rogalev, and J. Goulon, *Phys. Rev. B* **55**, 3663 (1997).

⁹T. Yang, B. X. Liu, F. Pan, J. Luo, and K. Tao, *J. Phys.: Condens. Matter* **7**, 1121 (1995).

¹⁰S. Blügel, B. Drittler, R. Zeller, and P. H. Dederichs, *Appl. Phys. A: Solids Surf.* **49**, 547 (1989).

¹¹T. Manago, H. Miyajima, K. Kawaguchi, M. Sohma, and I. Yamaguchi, *J. Magn. Magn. Mater.* **177-181**, 1191 (1998).

¹²T. Manago, T. Ono, H. Miyajima, K. Kawaguchi, and M. Sohma, *J. Phys. Soc. Jpn.* **68**, 334 (1999).

¹³T. Manago, T. Ono, H. Miyajima, K. Kawaguchi, and M. Sohma, *J. Phys. Soc. Jpn.* **68**, 3677 (1999).

¹⁴For a recent review see G. P. Felcher, *J. Appl. Phys.* **87**, 5431 (2000).

¹⁵L. G. Parratt, *Phys. Rev.* **95**, 359 (1954).

¹⁶G. P. Felcher, *Phys. Rev. B* **24**, 1595 (1981).

¹⁷As stated here the analysis is only correct if the magnetization is parallel with the applied magnetic field, which is sufficient for our measurements since they were done in large magnetic fields. A magnetization component perpendicular to the applied field gives rise to spin-flip scattering, which makes the analysis of the data more complex.

¹⁸G. P. Felcher, K. E. Gray, R. T. Kampwirth, and M. B. Brodsky, *Physica B & C* **136B**, 59 (1986).

¹⁹J. A. C. Bland, D. Pescia, and R. F. Willis, *Phys. Rev. Lett.* **58**, 1244 (1987).

²⁰M. R. Fitzsimmons, A. Röhl, E. Burkel, K. E. Sikafus, M. A. Nastasi, G. S. Smith, and R. Pynn, *J. Appl. Phys.* **76**, 6295 (1994).

²¹Even though matching of nuclear scattering length densities is

- demonstrated here for a specific combination of materials, it should be noted that in general there is enough distribution of scattering lengths for various isotopes so that this matching in principle is possible for many heterostructures.
- ²²A. L. Shapiro, F. Hellman, and M. R. Fitzsimmons, in *Proceedings of High-Density Magnetic Recording and Integrated Magneto-Optics: Materials and Devices Symposium, San Francisco, 1998*, edited by J. Bain, M. Levy, J. Lorenzo, T. Nolan, Y. Okamura, K. Rubin, B. Stadler, and R. Wolfe (Materials Research Society, Warrendale, 1998), p. 311.
- ²³While we did not see in-plane NiO peaks for this particular film due to its rather thin NiO layer of 46.5 Å, we did confirm good epitaxy for thicker NiO films.
- ²⁴C. Leighton, M. R. Fitzsimmons, P. Yashar, A. Hoffmann, J. Nogués, J. Dura, C. F. Majkrzak, and I. K. Schuller, *Phys. Rev. Lett.* **86**, 4394 (2001).
- ²⁵M. R. Fitzsimmons, A. Hoffmann, J. R. Groves, R. W. Springer, P. N. Arendt, C. Leighton, I. K. Schuller, K. Liu, J. Nogués, C. F. Majkrzak, J. A. Dura, V. Leiner, and H. Lauter (unpublished).
- ²⁶G. S. Smith and C. F. Majkrzak, in *International Tables for Crystallography, Volume C: Mathematical, Physical and Chemical Tables*, edited by A. J. C. Wilson and E. Prince (Kluwer Academic, Dordrecht, 1999), p. 126.
- ²⁷Y. Shimomura, M. Kojima, and S. Saito, *J. Phys. Soc. Jpn.* **11**, 1136 (1956).
- ²⁸H. Ohldag, A. Scholl, F. Nolting, S. Anders, and J. Stöhr (unpublished).
- ²⁹T. Ambrose and C. L. Chien, *Phys. Rev. Lett.* **76**, 1743 (1996).
- ³⁰R. H. Kodama, S. A. Makhlof, and A. E. Berkowitz, *Phys. Rev. Lett.* **79**, 1393 (1997).
- ³¹H. Komatsu and M. Ishigame, *J. Mater. Sci.* **20**, 4027 (1985).